*International Journal of Thermophysics, Vol. 27, No. 4, July 2006 (© 2006)*
DOI: 10.1007/s10765-006-0090-x

# A Multiparameter Viscosity Equation for 1,1-Difluoroethane (R152a) with an Optimized Functional Form[1]

**P. Marchi,[2] G. Scalabrin,[2,3] and M. Grigiante[4]**

This paper presents a new formulation for the viscosity surface of 1,1-difluoroethane (R152a). The formulation is a multiparameter equation $\eta = \eta(\rho, T)$ obtained from an optimization technique of the functional form based on available experimental data. The equation is valid for temperatures from 240 to 440 K and pressures up to 20 MPa. Two lines of viscosity minima have been observed, and they have been analytically defined. A high accuracy equation of state for R152a was used to convert the experimental variables $(P, T)$ into the independent variables of the viscosity equation $(\rho, T)$. Comparisons with data are given to establish the accuracy of the viscosity values calculated using this equation. The obtained results are very satisfactory with an average absolute deviation of 0.27% for the selected 264 primary data points, and this is a significant improvement with respect to other equations in the literature.

**KEY WORDS:** 1,1-difluoroethane; correlation techniques; multiparameter equations; R152a; transport properties; viscosity.

## 1. INTRODUCTION

The halofluorocarbon R152a (1,1-difluoroethane) is a refrigerant with a wide range of applications, and increasing utilization. It presents a

[1]Paper presented at the Seventeenth European Conference on Thermophysical Properties, September 5-8, 2005, Bratislava, Slovak Republic.

[2]Dipartimento di Fisica Tecnica, Università di Padova, via Venezia 1, I-35131 Padova, Italy.

[3]To whom correspondence should be addressed. Email: gscala@unipd.it

[4]Dipartimento di Ingegneria Civile Ambientale, Università di Trento, via Mesiano 77, I-38050 Trento, Italy.

null ozone-depletion potential (ODP) and a relatively low global-warming potential (GWP), which allow it to be accepted as an environmentally benign refrigerant. Due to the important engineering applications of this fluid, its thermodynamic and transport properties are of great interest.

Two different approaches can be found in the literature, to represent the viscosity surface of a fluid. The first approach includes predictive or semi-predictive models which are often based on corresponding states theory [1–10], and in many cases, they can be used to estimate the property with an accuracy level which is considered sufficient for engineering calculations. Theoretically based models, for instance, those including the evaluation of collision integrals, have also been developed. These types of models do not require experimental data. However, they are generally not as accurate as formulations based on experimental data. The second approach can be either semi-theoretically based or totally heuristic, and for both of these groups suitable models have been developed.

The group of semi-theoretically based models includes the present state-of-the-art technique for the development of viscosity equations, which is based on the residual concept superimposing three parts: the dilute-gas term, the excess term, and the critical enhancement term [11]. Though some functional forms obtained from theoretical analysis are included into the equations in this format, the technique requires experimental data as evenly distributed as possible over the whole $\eta\rho T$ surface and it is then to some extent correlative. It normally gives an equation of the form $\eta = \eta(T, \rho)$, where the viscosity $\eta$ depends on the temperature $T$ and on the density $\rho$. Since the viscosity data are related to the experimentally accessible variables, which are the temperature $T$ and the pressure $P$, an equation of state is required to convert $(T, P)$ into $(T, \rho)$. Moreover, the regression technique presents some difficulties as evidenced in Ref. 12. In the following, the viscosity models of this type will be referred to as "conventional equations" and for R152a an equation in this format was developed by Krauss et al. [13].

As an alternative to the conventional technique, totally heuristic methods have been studied and applied. Such an approach is strictly related to universal function approximators, i.e., mathematical models that express the analytical relation between dependent and independent variables directly from the experimental representation of the studied phenomenon. A number of viscosity models pertaining to this group has been developed, and they are based on multilayer feedforward neural networks [14–18], on a combination of the extended corresponding states and the neural networks technique [19, 20], and on an optimization algorithm of the functional form [12, 21].

In particular, the optimization technique for multiparameter equations of state, developed by Setzmann and Wagner [22], has been previously applied with satisfactory results to the viscosity modeling of R134a [12] and propane [21] and the same method is used here for R152a.

## 2. PROCEDURE FOR DEVELOPING AN EMPIRICAL EQUATION FOR VISCOSITY

### 2.1. Fitting a Multiparameter Empirical Equation

The viscosity surface of a fluid can be represented through an empirical equation in the form $\eta = \eta(T, \rho, \bar{n})$, where $\bar{n}$ represents the array of the individual coefficients that have to be fitted.

The calculation of the optimum set of values for the coefficients $\bar{n}$ is obtained by minimizing an objective function composed of a sum of squares $\chi^2$ as follows:

$$\chi^2(\bar{n}) = \sum_{i=1}^{N} \left( \frac{100}{u_{\%}} \frac{(\eta_{\text{exp}} - \eta_{\text{calc}}(\bar{n}))}{\eta_{\text{exp}}} \right)_i^2, \tag{1}$$

where $N$ is the total number of primary experimental points and the subscripts "exp" and "calc" stand for experimental and calculated values, respectively. The deviation of each experimental point from the equation is weighted using its experimental uncertainty $u_{\%}$, for which values can be obtained from the claimed uncertainties given by the experimenter.

The minimization technique developed by Setzmann and Wagner [22] is used for the present study. Starting from a large comprehensive function, the algorithm selects the functional form which yields the best representation of the selected experimental data with the simplest equation.

### 2.2. Bank of Terms

A comprehensive function, called "bank of terms" and composed of a total of 267 terms, is used for the optimization algorithm. This function is expressed in terms of dimensionless parameters, and can be written as

$$\eta_{\text{r}} = \sum_{i=0}^{10} \sum_{j=0}^{20} n_{ij} T_{\text{r}}^i \rho_{\text{r}}^j + \sum_{i=0}^{5} \sum_{j=0}^{5} n_{ij} T_{\text{r}}^i \rho_{\text{r}}^j e^{-\rho_{\text{r}}^2}, \tag{2}$$

**Table I.** Substance-Specific Parameters for the Target Fluid R152a

| | | Ref. |
|---|---|---|
| $M$ (kg·mol$^{-1}$) | 0.066051 | 25 |
| $T_c$ (K) | 386.41 | 25 |
| $P_c$ (MPa) | 4.5157 | 25 |
| $\rho_c$ (kg·m$^{-3}$) | 368.0 | 25 |
| $H_c$ ($\mu$Pa·s) | 21.6451 | – |

with

$$\begin{aligned} T_r &= T/T_c \\ \rho_r &= \rho/\rho_c \\ \eta_r &= \ln\left(\eta/H_c + 1\right), \\ H_c &= \frac{M^{1/2} P_c^{2/3}}{R^{1/6} N_A^{1/3} T_c^{1/6}} \end{aligned} \tag{3}$$

where the subscript "c" denotes a critical value. Since the viscosity diverges to infinity at the critical point, its critical value is substituted by the pseudo-critical viscosity $H_c$ that is obtained from dimensional analysis. In the definition of $H_c$, Eq. (3), the molar mass $M$ is expressed in kg·mol$^{-1}$, the critical temperature $T_c$ in K, and the critical pressure $P_c$ in Pa. Further parameters are the molar gas constant ($R = 8.314472\,\text{J·mol}^{-1}\text{·K}^{-1}$), taken from Ref. 23, and the Avogadro number ($N_A = 6.0221353 \times 10^{23}\,\text{mol}^{-1}$), taken from Ref. 24.

For the target fluid R152a, the values of the parameters involved in the former variable definitions are reported in Table I.

## 3. WIDE-RANGE MULTIPARAMETER VISCOSITY EQUATION

### 3.1. Experimental Data

An extensive literature search for the available viscosity experimental data sets of R152a has produced a total of 20 sources. They are listed in Table II in which the column "NPT" gives the number of experimental points for each data set. Table II reports the ranges of the independent variables and the adopted measurement method for each data source. The other parts of the table will be explained in the following.

In this work the temperatures were considered according to the International Temperature Scale of 1990 (ITS-90) [46]. Therefore, the temperatures of the experimental data measured according to older temperature scales were converted to ITS-90.

**Table II.** Experimental Data and Their Deviations from the New Viscosity Equation, Eq. (6), in Liquid, Vapor, and Supercritical Regions. Data are within Validity Limits of Eq. (6)

| Ref. | First author | Phase[a] | NPT | NPT range | $T$ range (K) | $P$ range (MPa) | Meas. method[b] | AAD (%) | Bias (%) | MAD (%) | Class | $u_{\%}$ (%) |
|---|---|---|---|---|---|---|---|---|---|---|---|---|
| *Liquid* | | | | | | | | | | | | |
| 26 | Assael | l | 32 | 32 | 273–333 | 1.4–17.7 | VW | 0.33 | 0.01 | 1.91 | I | 0.5 |
| 26 | Assael | sl | 7 | 7 | 273–333 | * | VW | 0.90 | 0.14 | 2.53 | I | 0.5 |
| 27, 28 | van der Gulik | sl | 35 | 35 | 243–373 | * | VW | 0.37 | −0.18 | 0.91 | I | 0.5 |
| | **Primary** | | | **74** | | | | **0.40** | **−0.07** | – | | |
| 29 | Arnemann | sl | 12 | 12 | 242–352 | * | RB | 3.10 | 1.47 | 9.36 | II | – |
| 30 | Fröba | sl | 14 | 14 | 243–373 | * | SLS | 2.87 | 0.76 | 7.92 | II | – |
| 31 | Heide | sl | 12 | 10 | 243–333 | * | FB | 3.51 | −3.38 | 11.29 | II | – |
| 32 | Kumagai | sl | 8 | 8 | 273–343 | * | CV | 2.31 | 1.27 | 6.38 | II | – |
| 33 | Kumagai | sl | 8 | 8 | 273–343 | * | CV | 3.32 | 0.94 | 8.68 | II | – |
| 34 | Kumagai | sl | 8 | 8 | 273–343 | * | CV | 2.25 | −2.25 | 2.79 | II | – |
| 35 | Mears | sl | 8 | 8 | 243–333 | * | CV | 26.88 | 26.88 | 39.08 | II | – |
| 36 | Phillips | sl | 9 | 6 | 245–318 | * | CV | 5.30 | 1.40 | 10.18 | II | – |
| 37 | Ripple | sl | 11 | 11 | 255–323 | * | CV | 3.25 | −3.25 | 5.37 | II | – |
| 38 | Sagaidakova | sl | 26 | 15 | 243–383 | * | C | 1.07 | −1.06 | 6.83 | II | – |
| | **Total** | | **190** | **174** | | | | **2.89** | **0.91** | – | | |
| *Vapor* | | | | | | | | | | | | |
| 39 | Assael | v | 21 | 21 | 275–333 | 0.2–1.2 | VW | 0.57 | −0.47 | 1.69 | I | 1.0 |
| 40 | Takahashi | v | 99 | 99 | 298–423 | 0.1–4.5 | OD | 0.13 | 0.02 | 0.38 | I | 0.5 |
| 41 | Takahashi | v | 49 | 49 | 273–303 | 0.1–0.7 | OD | 0.19 | 0.15 | 0.48 | I | 0.5 |
| 39 | Assael | sv | 7 | 7 | 273–333 | * | VW | 0.46 | 0.08 | 0.69 | I | 1.0 |
| | **Primary** | | | **176** | | | | **0.21** | **0.00** | – | | |

**Table II.** (*Continued*)

| Ref. | First author | Phase[a] | NPT | NPT range | $T$ range (K) | $P$ range (MPa) | Meas. method[b] | AAD (%) | Bias (%) | MAD (%) | Class | $u_{\%}$ (%) |
|---|---|---|---|---|---|---|---|---|---|---|---|---|
| 42 | Mayinger | v | 332 | 218 | 253–433 | 0.1–4.5 | OD | 1.47 | 1.37 | 14.82 | II | – |
| 43 | Nagaoka | v | 2 | 2 | 298–323 | 0.1–0.1 | RB | 0.81 | 0.81 | 1.26 | II | – |
| 44 | Schramm | v | 11 | 8 | 250–423 | 0.1–0.1 | C | 0.68 | −0.68 | 1.18 | II | – |
| 42 | Mayinger | sv | 12 | 12 | 253–363 | * | OD | 2.95 | 2.66 | 13.28 | II | – |
| 42 | Mayinger | sv | 12 | 12 | 249–386 | * | OD | 6.00 | 5.73 | 25.57 | II | – |
| 45 | Takahashi | sv | 19 | 19 | 294–386 | * | OD | 2.89 | −2.27 | 11.24 | II | – |
| 27, 28 | van der Gulik | sv | 36 | 36 | 243–373 | * | VW | 6.43 | 4.40 | 20.15 | II | – |
| | **Total** | | **600** | **483** | | | | **1.56** | **1.06** | – | | |
| *Supercritical region* | | | | | | | | | | | | |
| 40 | Takahashi | sc | 14 | 14 | 398–423 | 4.5–5.3 | OD | 0.29 | −0.02 | 0.47 | I | 0.5 |
| | **Primary** | | | **14** | | | | **0.29** | **−0.02** | – | | |
| 42 | Mayinger | sc | 63 | 15 | 393–433 | 5.0–8.0 | OD | 12.10 | 12.10 | 26.57 | II | – |
| | **Total** | | **77** | **29** | | | | **6.40** | **6.25** | – | | |
| *Generated data* | | | | | | | | | | | | |
| **Near-critical generated data** | | | | **13** | | | | **0.71** | **−0.07** | **1.16** | | |
| *Overall* | | | | | | | | | | | | |
| **Overall primary** | | | – | **264** | | | | **0.27** | **−0.02** | – | | |
| **Overall** | | | **867** | **686** | | | | **2.10** | **1.24** | – | | |

[a] Phase: l = liquid, sl = saturated liquid, v = vapor, sv = saturated vapor, sc = supercritical.

[b] Measurement method: C = calculated, CV = capillary viscometer, FB = falling ball viscometer, OD = oscillating disk viscometer, RB = rolling ball viscometer, SLS = surface light scattering, VW = vibrating wire viscometer.

### 3.2. Screening Procedure and Primary Data Sets

The viscosity data available from the literature cannot be used for the equation development without a suitable screening on the basis of their experimental quality. The screening was performed according to the following procedure.

Since a viscosity equation for R152a is available in the conventional format [13], it was used to preliminarily screen the data within the validity range of the equation. All the available data sets were considered, even those that were published after the development of the conventional equation.

For each experimental point the error deviation $\Delta$ with respect to the equation was calculated as

$$\Delta = \frac{\eta_{\text{exp}} - \eta_{\text{calc}}}{\eta_{\text{exp}}}. \tag{4}$$

The following statistical indexes, which are used throughout the present work, were evaluated from the error deviations $\Delta$: the average absolute deviation (AAD), the bias, and the maximum absolute deviation (MAD). These are defined as

$$\text{AAD}\,(\%) = \frac{100}{\text{NPT}} \sum_{i=1}^{\text{NPT}} |\Delta|_i \quad \text{Bias}\,(\%\ ) = \frac{100}{\text{NPT}} \sum_{i=1}^{\text{NPT}} (\Delta)_i$$
$$\text{MAD}\,(\%) = 100 \underset{i=1,\text{NPT}}{\text{Max}} |\Delta|_i \tag{5}$$

Each data set was evaluated as a whole because it was assumed that all the data from a given set were obtained with a consistent accuracy. An error threshold with respect to the conventional equation was selected at an AAD of 5%. The data sets from this first screening compose the *preliminary* sources. The *preliminary data* are obtained including all the points of the preliminary sources; also included are those that are outside the validity range of the conventional viscosity equation.

A first regression was developed on the preliminary data with the optimization algorithm. An initial selection of the primary data sets was obtained considering only the data with a threshold of 2 to 3% for the AAD and a low value of the bias.

These data were further screened through regressions with the optimization algorithm thus refining the choice of the so-called primary data sets. During this procedure some sets were moved from primary to secondary and *vice-versa*, searching for the AAD of the single sets close to the overall value for the primary data, and for the bias values close to zero. The aim of the procedure was to gather those sets with the lowest error

deviations and statistically centered as much as possible with respect to the multiparameter viscosity equation.

The screening led to a stable selection of primary data on which the final version of the multiparameter equation was regressed. In Table II the primary data sets are indicated with the symbol I, whereas the secondary with II. The ascribed uncertainties $u_{\%}$ for the primary sets are given in the last column of Table II. The distribution of the primary data on a $P, T$ plane is shown in Fig. 1.

### 3.3. Near-Critical Region

The fluid R152a has a very limited number of experimental points in the near-critical region, and this results in a lack of information about the trend of the viscosity surface in the region where a strong variation of the viscosity derivatives with respect to the independent variables is expected. The heuristic modeling procedure requires a number of points with a rather regular distribution in that region in order to allow the model to follow the characteristic trends close to the critical region.

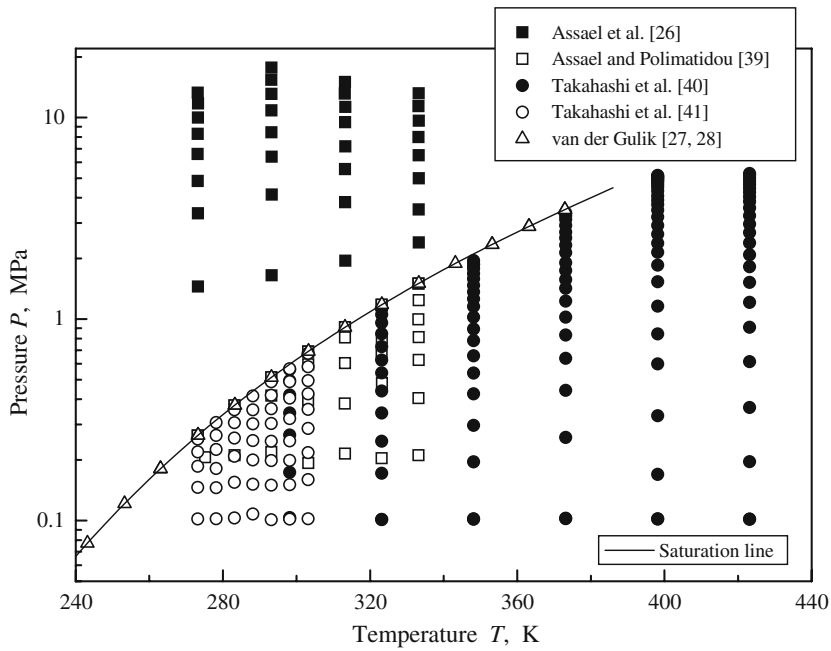


**Fig. 1.** Distribution of the data selected as primary data.

Since data in this region are sparse, pseudo-experimental data were generated using the conventional viscosity equation [13], in which a critical enhancement following the Olchowy and Sengers theory [47, 48] is included, and a total of 13 points distributed as shown in Fig. 2 was produced. In this figure the isotherms and the saturation curve are from the conventional equation [13]. These data have been used as primary data for the regression of the new viscosity equation. The goal of using the pseudo-experimental data is to obtain a correct physical trend but not to assure a documented accuracy for the equation in the near-critical region.

The critical enhancement for viscosity has an influence limited to a very narrow region centered on the critical point, where the viscosity approaches an infinity limit. In this work the modeling of the critical enhancement was omitted.

### 3.4. New Equation for the Viscosity of R152a

Assuming the final selection of the primary data sets, an equation in the form $\eta = \eta(T, \rho)$ was obtained from the optimization procedure. This resulting equation is

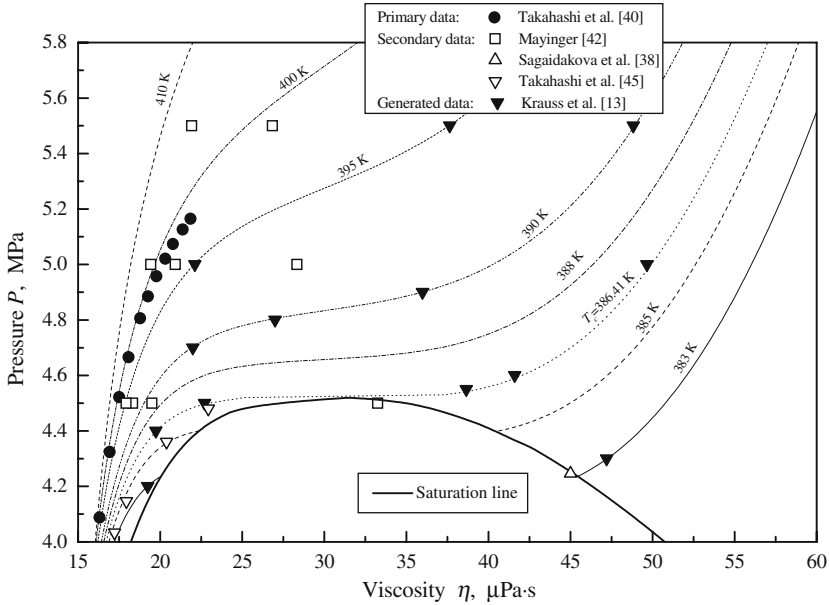


**Fig. 2.** Representation of experimental and generated data in the near-critical region.

$$\eta_r = \sum_{i=1}^{9} n_i T_r^{g_i} \rho_r^{h_i} + e^{-\rho_r^2} \sum_{i=10}^{14} n_i T_r^{g_i} \rho_r^{h_i} \tag{6}$$

with the coefficients, exponents, and validity limits reported in Table III.

The extrapolation of Eq. (6) outside the validity limits, particularly at low temperatures and at high pressures, is not accurate and it may result in rather unreliable values. In Fig. 1 it can be seen that the primary data do not regularly fill all the regions of the stated validity range, but we chose to assume a rectangular contour for its boundaries. This assumption will be discussed further in Section 5.3.

The development of a viscosity equation in the form $\eta = \eta(T, \rho)$ requires a conversion of experimental data from $(T, P)$ to $(T, \rho)$ variables. The R152a equation of state by Tillner-Roth [25] was used for this purpose. Some viscosity values generated from Eq. (6) are reported in Table IV, which can be used by the reader for checking a computer code.

## 4. VALIDATION OF THE NEW VISCOSITY EQUATION

A detailed validation with respect to both primary and secondary data has been developed for the new viscosity equation and the results are

**Table III.** Parameters of Eq. (6) and Validity Limits

| $i$ | $g_i$ | $h_i$ | $n_i$ |
|---|---|---|---|
| 1 | 0 | 2 | 1.14230266 |
| 2 | 0 | 3 | −1.56310931 |
| 3 | 0 | 4 | 0.481682618 |
| 4 | 0 | 18 | $0.208435890 \times 10^{-7}$ |
| 5 | 1 | 1 | 1.18637350 |
| 6 | 1 | 14 | $-0.493635860 \times 10^{-5}$ |
| 7 | 2 | 0 | $-0.985341189 \times 10^{-1}$ |
| 8 | 5 | 12 | $-0.584922887 \times 10^{-4}$ |
| 9 | 7 | 20 | $0.354808573 \times 10^{-7}$ |
| 10 | 0 | 1 | −0.997534105 |
| 11 | 1 | 0 | 0.581028512 |
| 12 | 4 | 1 | −0.176909131 |
| 13 | 4 | 4 | 1.90889418 |
| 14 | 5 | 4 | −2.06373190 |
| Validity limits | | | |
| $T$ (K) | | | 240–440 |
| $P$ (MPa) | | | $\leq 20$ |

**Table IV.** Viscosity Values Generated from Eq. (6)

| $T$ (K) | $P$ (MPa) | $\rho$ (kg·m$^{-3}$) | $\eta$($\mu$Pa·s) |
|---|---|---|---|
| 240 | 0.1 | 1029.631 | 362.376 |
| 298.15 | 0.1 | 2.72166 | 10.2802 |
| 340 | 0.1 | 2.3673 | 11.7824 |
| 440 | 0.1 | 1.81493 | 15.2809 |
| 300 | 1 | 895.93 | 161.472 |
| 350 | 3 | 748.196 | 92.42 |
| 400 | 5 | 207.449 | 19.5811 |
| 350 | 10 | 803.522 | 114.95 |
| 250 | 15 | 1034.833 | 351.248 |
| 440 | 20 | 631.041 | 60.2984 |

reported in Table II. The column denoted by "NPT range" gives the number of data within the validity limits of the equation for each data set.

The representation of the error deviations of the new viscosity equation with respect to each point of the primary data set is shown in the $P, T$ diagram of Fig. 3 where the size of the symbols indicates the magnitude of each deviation.

Furthermore, the deviations between Eq. (6) and all the primary data are represented in Fig. 4 as a function of pressure, for several steps of temperature. The dashed lines represent the deviation of Eq. (6) with respect to the conventional equation from Krauss et al. [13]; for each figure the temperature of the comparison between the two equations was taken at the mean value of the indicated range.

Considering the deviations from the data and their claimed experimental uncertainties, the accuracy of the present viscosity equation is estimated to be 0.25% for the vapor phase and the region at pressures lower than the critical value, and 0.5% for the liquid phase. Since very few primary data are available in the liquid at temperatures greater than 350 K and in the supercritical region, in these regions the accuracy is cautiously set at 1%.

## 5. BEHAVIOR OF THE VISCOSITY SURFACE

### 5.1. Representation of the Viscosity Surface on a $T$, $\eta$ Plane

Some isobars and the vapor side of the saturation curve obtained from the new viscosity equation are plotted in Fig. 5 on a $T, \eta$ plane. A line of viscosity minima in the dense-gas region is observed.

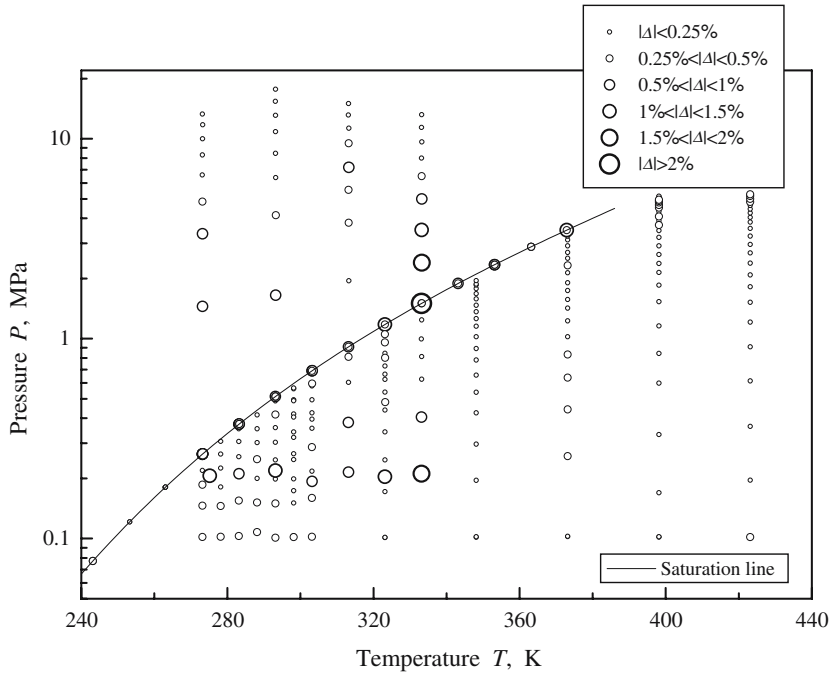


**Fig. 3.** Deviations between all primary experimental data and values calculated from Eq. (6) shown in a $P$, $T$ diagram.

Within the range of validity of the equation, the viscosity minima are found in the pressure range $2.815 \leq P/\text{MPa} \leq 5.195$, that is, $0.623 \leq P_r \leq 1.150$, as shown in Fig. 5. The locus of the minima can be represented by the function:

$$y = a + bx + cx^2 \tag{7}$$

for which the variables and the corresponding parameters are given in Table V.

### 5.2. Representation of the Viscosity Surface on a *P*, $\eta$ Plane

The plot of isotherms calculated from Eq. (6) is shown on a $P, \eta$ plane in Fig. 6, and a magnified part in the vapor region close to the critical point is also shown in Fig. 7. The shape of the surface in that

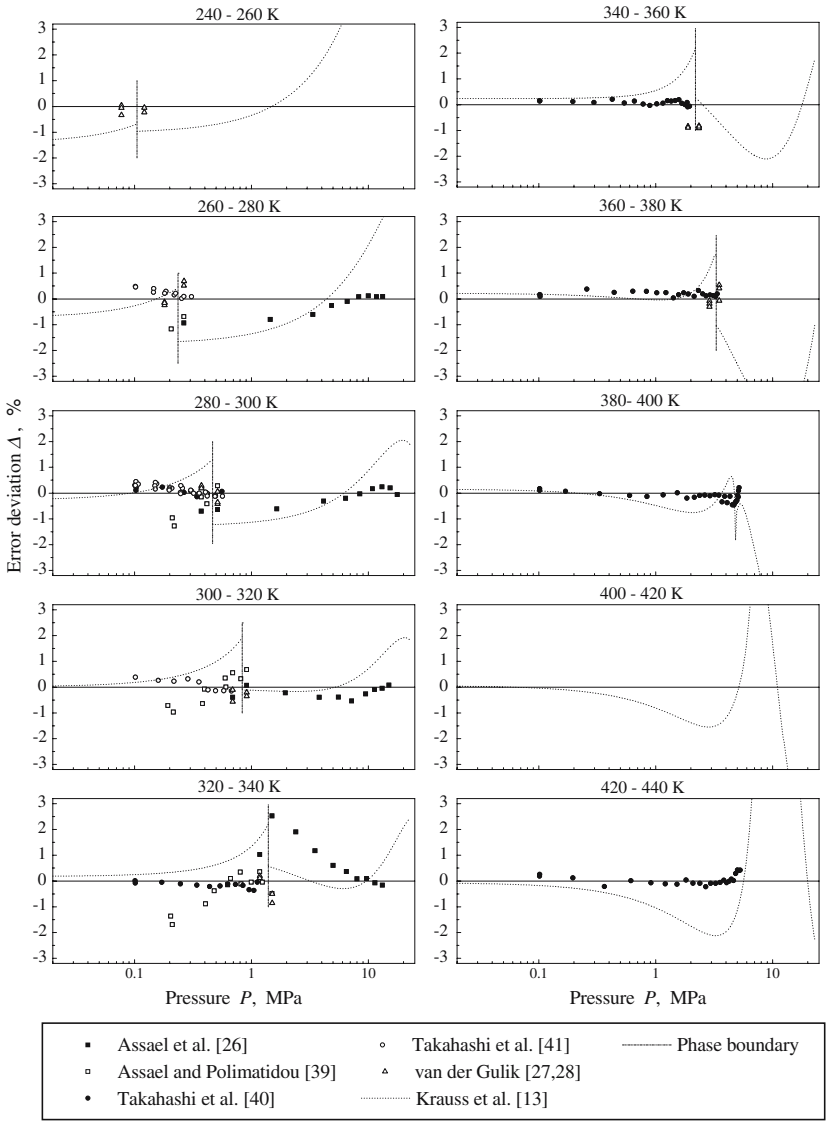


**Fig. 4.** Deviations between all experimental points in the primary data sets and Eq. (6), sorted by temperature. Plotted lines correspond to values calculated from the conventional equation by Krauss et al. [13].

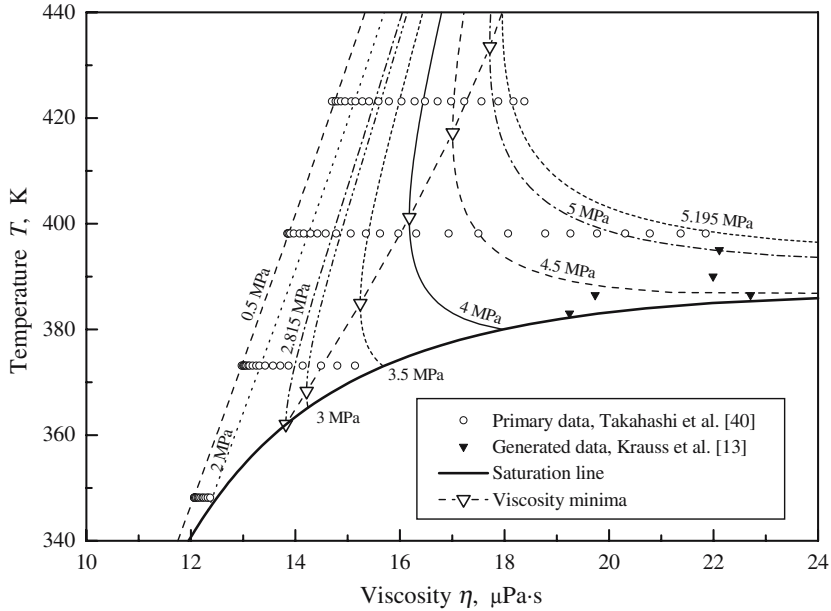


**Fig. 5.** Isobars and saturated-vapor line calculated from Eq. (6) and plotted on a $T, \eta$ plane. Viscosity minima are observed in the dense-gas phase.

**Table V.** Variables and Parameters of Eq. (7) for the Locus of the Viscosity Minima Found along Isobars

| $x$ | $y$ | $a$ | $b$ | $c$ |
|---|---|---|---|---|
| $P_r$ | $T_r$ | 0.691953 | 0.399560 | −0.00997770 |
| $P_r$ | $\rho_r$ | 0.0697750 | 0.447877 | −0.165814 |
| $P_r$ | $\eta_r$ | 0.264764 | 0.452253 | −0.136622 |

region exhibits correct trends of the isotherms close to the critical isotherm, based upon the hypothesis of neglecting the very narrow range around the critical point where the contribution of the viscosity critical enhancement is significant.

The new viscosity equation in the region of low-density vapor is represented on a $P, \eta$ plane in Fig. 8. A line of viscosity minima is observed in the temperature range $304 \leq T/\mathrm{K} \leq 377.25$, that is, $0.787 \leq T_r \leq 0.976$,

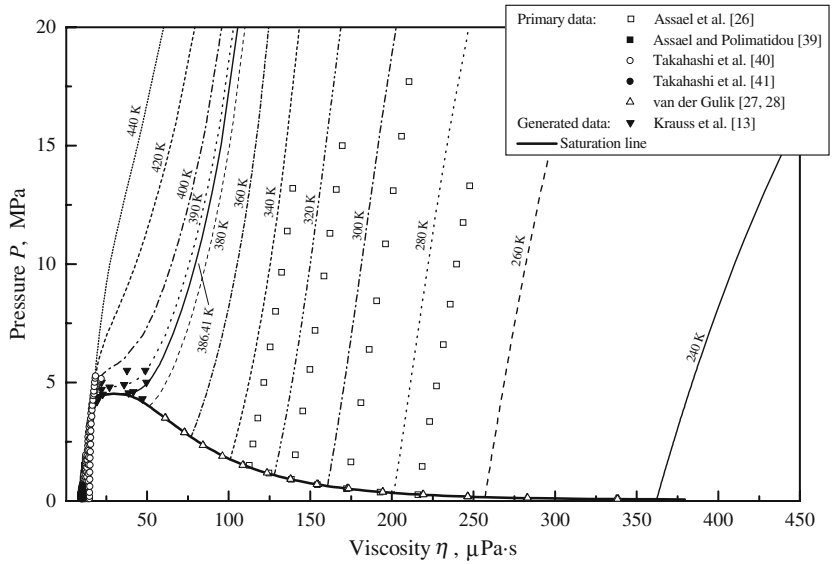


**Fig. 6.** Isotherms and saturation curve calculated from Eq. (6) and plotted on a $P, \eta$ plane.

**Table VI.** Variables and Parameters of Eq. (7) for the Locus of the Viscosity Minima Found along Isotherms in the Low-Density Vapor Region

| $x$ | $y$ | $a$ | $b$ | $c$ |
|---|---|---|---|---|
| $T_r$ | $P_r$ | 0.140673 | 0.717766 | −0.884079 |
| $T_r$ | $\rho_r$ | 0.635896 | −1.067948 | 0.426690 |
| $T_r$ | $\eta_r$ | −0.169060 | 0.933614 | −0.282384 |

and it can be represented by the functional form of Eq. (7), but with the variables and coefficients from Table VI.

### 5.3. Discussion on the Validity Limits

In Section 3.4 the validity limits of the new viscosity equation, Eq. (6), were briefly discussed. The preceding plots make evident that the primary data do not uniformly fill a single regular range, both in temperature and in pressure. Therefore, for the sake of precision, an irregular contour for the validity range should be selected. In fact in Fig. 6 one can see a lack of data for liquid states at $T < 270\,\mathrm{K}$ and $T > 340\,\mathrm{K}$, whereas in Fig. 8

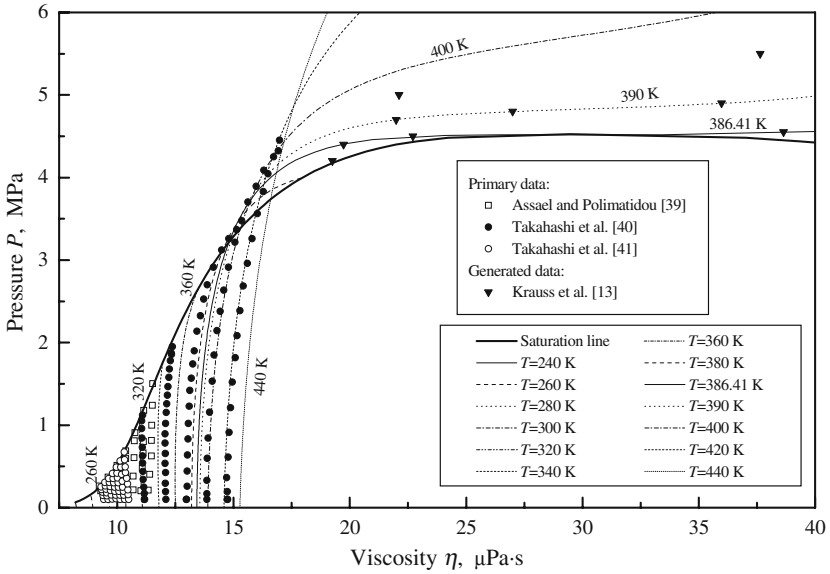


**Fig. 7.** Isotherms and saturation curve calculated from Eq. (6) and plotted on a $P, \eta$ plane for the vapor phase close to the critical point.

data for the vapor phase are not available at $T < 270\,\mathrm{K}$. For the supercritical region data are not available at $P > 5.3\,\mathrm{MPa}$. Similar comments can be drawn from Fig. 1.

However, the plots of viscosities from the new equation together with the experimental points, in particular, Figs. 6 and 8, indicate that the trends of the new equation in the areas where experimental points are not available are regular and correspond well to the expected behavior. For these reasons the validity range in the $P$, $T$ plane is taken as a rectangular shape bounded by temperature of 240 and 440 K at pressures up to 20 MPa. Slightly increased uncertainties may occur when the equation is applied within the limits of the validity range in areas where there are no primary data available, because the equation accuracy cannot be verified without experimental data.

## 6. COMPARISON WITH THE CONVENTIONAL EQUATION

The conventional viscosity equation published in the literature [13] was used for comparison. The density entering this equation was calcu-

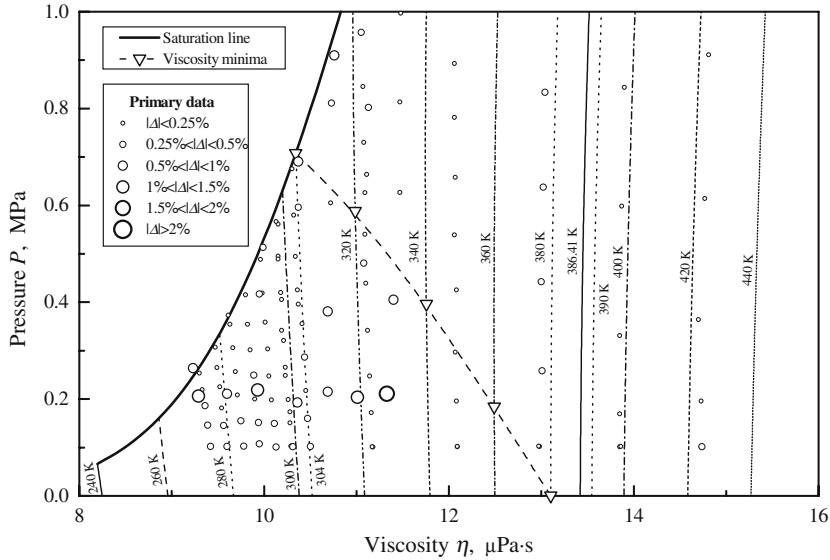


**Fig. 8.** Isotherms and saturated-vapor line calculated from Eq. (6), plotted on a $P, \eta$ plane. Viscosity minima are observed along a line in the low-density gas region.

lated from the $T$, $P$ values using the equation of state of Tillner-Roth [25]; the crossover model of van Pelt and Sengers [49] was assumed for the near-critical region as in the original publication [13]. The validity range of this conventional equation is the same of that of the present viscosity equation.

Considering only the primary data, Eq. (6) is significantly superior to the conventional equation for both the single regions and the whole surface, as the AAD and Bias values shown in Table VII. A significant difference is found in particular for the vapor region: the present equation exhibits an excellent behavior, whereas the conventional one has a higher AAD and a large Bias, indicating that it is shifted with respect to the data. Also in the liquid and supercritical regions the AAD values with respect to data are far lower for the new equation.

The deviations between the conventional equation and the primary experimental data are shown in Fig. 9, which corresponds to Fig. 3 for the present equation.

**Table VII.** Statistical Analysis of the Representation of the Primary Data Set by Eq. (6) and by the Conventional Equation of Krauss et al. [13]. Data are within the Validity Limits of Eq. (6)

| | | | | Equation (6) | | | Krauss et al. equation [13] | | | |
|---|---|---|---|---|---|---|---|---|---|---|
| Ref. | First author | Phase | NPT | AAD (%) | Bias (%) | MAD (%) | AAD (%) | Bias (%) | MAD (%) | Class Eq. (6) |
| *Liquid* | | | | | | | | | | |
| 26 | Assael | l | 32 | 0.33 | 0.01 | 1.91 | 0.90 | −0.49 | 2.71 | I |
| 26 | Assael | sl | 7 | 0.90 | 0.14 | 2.53 | 0.66 | 0.66 | 1.96 | I |
| 27, 28 | van der Gulik | sl | 35 | 0.37 | −0.18 | 0.91 | 0.93 | 0.37 | 2.32 | I |
| | **Primary** | | **74** | **0.40** | **−0.07** | – | **0.89** | **0.02** | – | |
| 29 | Arnemann | sl | 12 | 3.10 | 1.47 | 9.36 | 3.26 | 2.02 | 9.19 | II |
| 30 | Fröba | sl | 14 | 2.87 | 0.76 | 7.92 | 2.92 | 1.24 | 7.81 | II |
| 31 | Heide | sl | 10 | 3.51 | −3.38 | 11.29 | 2.71 | −2.71 | 11.17 | II |
| 32 | Kumagai | sl | 8 | 2.31 | 1.27 | 6.38 | 1.74 | 1.68 | 5.94 | II |
| 33 | Kumagai | sl | 8 | 3.32 | 0.94 | 8.68 | 2.54 | 1.36 | 8.25 | II |
| 34 | Kumagai | sl | 8 | 2.25 | −2.25 | 2.79 | 1.84 | −1.84 | 2.41 | II |
| 35 | Mears | sl | 8 | 26.88 | 26.88 | 39.08 | 27.17 | 27.17 | 38.73 | II |
| 36 | Phillips | sl | 6 | 5.30 | 1.40 | 10.18 | 5.49 | 2.23 | 9.94 | II |
| 37 | Ripple | sl | 11 | 3.25 | −3.25 | 5.37 | 2.48 | −2.48 | 4.06 | II |
| 38 | Sagaidakova | sl | 15 | 1.07 | −1.06 | 6.83 | 1.28 | −0.53 | 6.72 | II |
| | **Total** | | **174** | **2.89** | **0.91** | – | **2.99** | **1.27** | – | |
| *Vapor* | | | | | | | | | | |
| 39 | Assael | v | 21 | 0.57 | −0.47 | 1.69 | 1.30 | −1.30 | 2.03 | I |
| 40 | Takahashi | v | 99 | 0.13 | 0.02 | 0.38 | 0.77 | −0.04 | 2.21 | I |
| 41 | Takahashi | v | 49 | 0.19 | 0.15 | 0.48 | 0.58 | −0.41 | 1.87 | I |
| 39 | Assael | sv | 7 | 0.46 | 0.08 | 0.69 | 1.54 | −1.54 | 2.77 | I |
| | **Primary** | | **176** | **0.21** | **0.00** | – | **0.81** | **−0.35** | – | |
| 42 | Mayinger | v | 218 | 1.47 | 1.37 | 14.82 | 1.52 | 1.49 | 13.33 | II |
| 43 | Nagaoka | v | 2 | 0.81 | 0.81 | 1.26 | 0.64 | 0.64 | 1.15 | II |

| | | | | | | | | | | |
|---|---|---|---|---|---|---|---|---|---|---|
| 44 | Schramm | v | 8 | 0.68 | −0.68 | 1.18 | 0.63 | −0.63 | 0.88 | II |
| 42 | Mayinger | sv | 12 | 2.95 | 2.66 | 13.28 | 1.59 | 1.25 | 11.44 | II |
| 42 | Mayinger | sv | 12 | 6 | 5.73 | 25.57 | 4.48 | 4.15 | 21.26 | II |
| 45 | Takahashi | sv | 19 | 2.89 | −2.27 | 11.24 | 4.31 | −4.31 | 15.68 | II |
| 27, 28 | van der Gulik | sv | 36 | 6.43 | 4.40 | 20.15 | 7.19 | 3.00 | 21.04 | II |
| | **Total** | | **483** | **1.56** | **1.06** | – | **1.85** | **0.72** | – | |
| *Supercritical* | | | | | | | | | | |
| 40 | Takahashi | sc | 14 | 0.29 | −0.02 | 0.47 | 0.77 | 0.07 | 1.37 | I |
| | **Primary** | | **14** | **0.29** | **−0.02** | – | **0.77** | **0.04** | – | |
| 42 | Mayinger | sc | 15 | 12.10 | 12.10 | 26.57 | 10.86 | 10.86 | 17.74 | II |
| | **Total** | | **29** | **6.40** | **6.25** | – | **5.99** | **5.65** | – | |
| *Overall* | | | | | | | | | | |
| | **Overall primary** | | **264** | **0.27** | **−0.02** | – | **0.83** | **−0.23** | – | |
| | **Overall** | | **686** | **2.10** | **1.24** | – | **2.31** | **1.07** | – | |

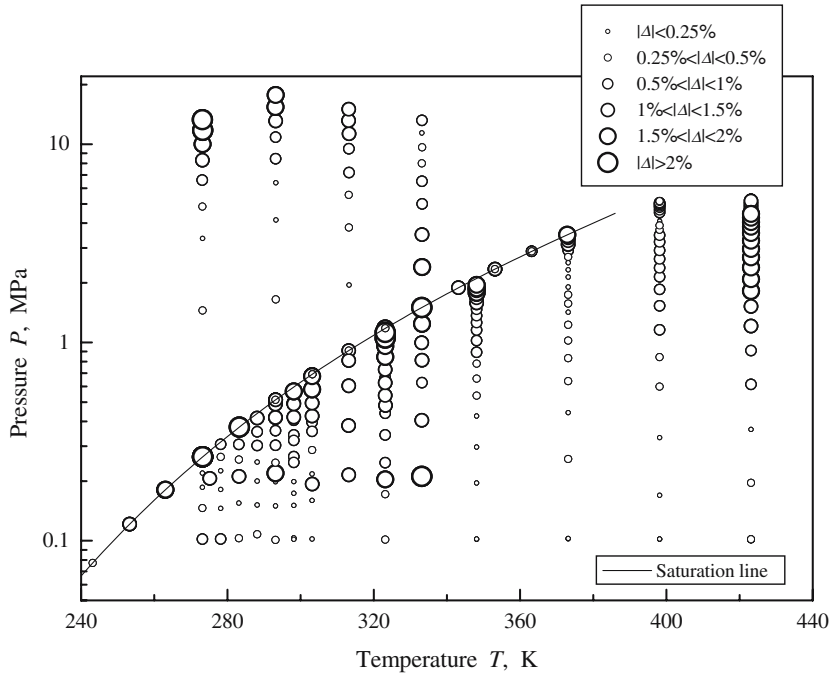


**Fig. 9.** Deviations of the conventional equation from Krauss et al. [13] with respect to each experimental point of the primary data sets.

## 7. CONCLUSIONS

A viscosity equation with a wide range of validity has been proposed for R152a. The adopted modeling method is based on the technique for the optimization of the functional form by Setzmann and Wagner [22] for the development of multiparameter equations of state. This method, completely correlative and directly based on the available experimental data, has been applied here as a function approximator for the viscosity surface. Considering the heuristic and non-theoretical nature of the modeling technique, this can be used as a powerful tool for screening the experimental data.

Even though the experimental data base available for the present fluid is not as large as those for other fluids studied with the same procedure, e.g., R134a [12] and propane [21], the performance of the new viscosity equation with respect to the primary data is of high quality. The new equation represents the primary data with an AAD of 0.27%. This is a sig-

nificant improvement over the AAD of 0.83% for the conventional equation [13] for the same database.

The estimated uncertainty of the equation is 0.25% for the vapor phase and the region at pressures lower than the critical value, 0.5% for the liquid phase, and 1% for the liquid region at temperatures greater than 350 K and in the supercritical region.

The functional form optimization procedure by Setzmann and Wagner is a promising tool for viscosity equation development, because it is able to represent the entire viscosity surface (except the critical region) well within the uncertainty of the experimental data.

Two loci of minima on the viscosity surface have been observed studying the behavior of the new equation in the low-density vapor region and the dense-fluid region near the supercritical conditions. Both lines of minima have been analytically represented.

At present this equation is the most accurate representation of the viscosity surface of R152a. Future experimental work investigating the regions not fully represented by data could allow a refinement and an extension of the equation reported here.

## REFERENCES

1. A. S. Teja and P. A. Thurner, *Chem. Eng. Commun*. **49**:79 (1986).
2. B. Willman and A. S. Teja, *Chem. Eng. J*. **37**:65 (1988).
3. K. J. Okeson and R. L. Rowley, *Int. J. Thermophys*. **12**:119 (1991).
4. G. Scalabrin and M. Grigiante, *Proc. 13th Symp. Thermophys. Prop.* (CD-ROM), Boulder, Colorado (1997).
5. G. Cristofoli, M. Grigiante, and G. Scalabrin, *High Temp.-High Press*. **33**:83 (2001).
6. G. Scalabrin, G. Cristofoli, and M. Grigiante, *Int. J. Energy Res.* **26**:1 (2002).
7. J. F. Ely and H. J. M. Hanley, *Ind. Eng. Chem. Fundam*. **20**:323 (1981).
8. M. L. Huber and J. F. Ely, *Fluid Phase Equilib.* **80**:239 (1992).
9. S. A. Klein, M. O. McLinden, and A. Laesecke, *Int. J. Refrig*. **30**:2089 (1997).
10. M. O. McLinden, S. A. Klein, E. W. Lemmon, and A. P. Peskin, *NIST Standard Reference Database 23, Version 6.0* (REFPROP) (1998).
11. J. Millat, J. H. Dymond, and C. A. Nieto de Castro, *Transport Properties of Fluids. Their Correlation, Prediction and Estimation* (Cambridge University Press, Cambridge, 1996).
12. G. Scalabrin, P. Marchi, and R. Span, *J. Phys. Chem. Ref. Data* **35**:839 (2006).
13. R. Krauss, V. C. Weiss, T. A. Edison, J. V. Sengers, and K. Stephan, *Int. J. Thermophys*. **17**:731 (1996).
14. G. Scalabrin, C. Corbetti, and G. Cristofoli, *Int. J. Thermophys*. **22**:1383 (2001).
15. G. Cristofoli, L. Piazza, and G. Scalabrin, *Fluid Phase Equilib.* **199**:223 (2002).
16. G. Scalabrin, L. Piazza, and V. Vesovic, *High Temp.-High Press*. **34**:457 (2002).
17. G. Scalabrin and G. Cristofoli, *Int. J. Refrig*. **26**:302 (2003).
18. G. Scalabrin and G. Cristofoli, *Int. J. Thermophys*. **24**:1241 (2003).
19. G. Scalabrin, G. Cristofoli, and D. Richon, *Fluid Phase Equilib.* **199**:265 (2002).
20. G. Scalabrin, G. Cristofoli, and D. Richon, *Fluid Phase Equilib.* **199**:281 (2002).

21. G. Scalabrin, P. Marchi, and R. Span, *J. Phys. Chem. Ref. Data* (in press).
22. U. Setzmann and W. Wagner, *Int. J. Thermophys*. **10**:1103 (1989).
23. P.J. Mohr and B. N. Taylor, *Rev. Mod. Phys.* **72**:351 (2000).
24. P. Becker, H. Bettin, H.-U. Danzebrink, M. Glaser, U. Kuetgens, A. Nicolaus, D. Schiel, P. De Bievre, S. Valkiers, and P. Taylor, *Metrologia* **40**: 271 (2003).
25. R. Tillner-Roth, *Int. J. Thermophys*. **16**:91 (1995).
26. M. J. Assael, S. K. Polimatidou, E. Vogel, and W. A. Wakeham, *Int. J. Thermophys*. **15**:575 (1994).
27. P. S. van der Gulik, *Int. J. Thermophys*. **14**:851 (1993).
28. P. S. van der Gulik, *Int. J. Thermophys*. **16**:867 (1995).
29. A. Arnemann and H. Kruse, *Proc. Int. Congr. Refrig*. (18) (Montréal, 1991), p. 379.
30. A. P. Fröba, S. Will, and A. Leipertz, *Int. J. Thermophys*. **21**:122 (2000).
31. R. Heide, *DKV-Tagungsbericht* (Leipzig, 1996), Vol. 23, p. 225.
32. A. Kumagai and S. Takahashi, *Int. J. Thermophys*. **12**:105 (1991).
33. A. Kumagai and S. Takahashi, *Proc. 8th Japan Symp. Thermophys. Prop*. (1987), p. 129.
34. A. Kumagai and C. Yokoyama, *Int. J. Thermophys*. **21**:909 (2000).
35. W. H. Mears, R. F. Stahl, S. R. Orfeo, R. C. Shair, L. F. Kells, W. Thompson, and H. McCann, *Ind. Eng. Chem.* **47**:1449 (1955).
36. T. W. Phillips and K. P. Murphy, *ASHRAE Trans*. **76**:146 (1970).
37. D. Ripple and D. Defibaugh, *J. Chem. Eng. Data* **42**:360 (1997).
38. N. G. Sagaidakova, V. A. Rykov, and T. N. Tsuranova, *Kholod. Tekh.* **5**:59 (1990).
39. M. J. Assael and S. K. Polimatidou, *Int. J. Thermophys*. **18**:353 (1997).
40. M. Takahashi, C. Yokoyama, and S. Takahashi, *J. Chem. Eng. Data* **32**:98 (1987).
41. M. Takahashi, C. Yokoyama, and S. Takahashi, *Nippon Reito Kyokai Ronb. (Trans. JAR)* **4**:25 (1987).
42. F. Mayinger, *DFG-Forschungsvorhaben, Abschulussbericht* (1991).
43. K. Nagaoka, Y. Yamashita, Y. Tanaka, H. Kubota, and T. Makita, *J. Chem. Eng. Japan* **19**:263 (1986).
44. B. Schramm, J. Hauck, and L. Kern, *Ber. Bunsenges. Phys. Chem*. **96**:745 (1992).
45. M. Takahashi, C. Yokoyama, and S. Takahashi, *Proc. 7th Japan Symp. Thermophys. Prop.* (1986), p. 179.
46. H. Preston-Thomas, *Metrologia* **27**:3 (1990).
47. G. A. Olchowy and J. V. Sengers, *Phys. Rev. Lett.* **61**:15 (1988).
48. G. A. Olchowy and J. V. Sengers, *Int. J. Thermophys*. **10**:417 (1989).
49. A. van Pelt and J. V. Sengers, *J. Supercrit. Fluids* **8**:81 (1995).